



Effect of an enhanced rubber-cement matrix interface on freeze-thaw resistance of the cement-based composite

Ngoc Phuong Pham, A. Toumi, Anaclet Turatsinze

► To cite this version:

Ngoc Phuong Pham, A. Toumi, Anaclet Turatsinze. Effect of an enhanced rubber-cement matrix interface on freeze-thaw resistance of the cement-based composite. *Construction and Building Materials*, 2019, 207, pp.528-534. 10.1016/j.conbuildmat.2019.02.147 . hal-02161732

HAL Id: hal-02161732

<https://hal.insa-toulouse.fr/hal-02161732>

Submitted on 22 Oct 2021

HAL is a multi-disciplinary open access archive for the deposit and dissemination of scientific research documents, whether they are published or not. The documents may come from teaching and research institutions in France or abroad, or from public or private research centers.

L'archive ouverte pluridisciplinaire **HAL**, est destinée au dépôt et à la diffusion de documents scientifiques de niveau recherche, publiés ou non, émanant des établissements d'enseignement et de recherche français ou étrangers, des laboratoires publics ou privés.



Distributed under a Creative Commons Attribution - NonCommercial 4.0 International License

1 Effect of an enhanced rubber-cement matrix interface on
2 freeze-thaw resistance of the cement-based composite

3 N-P. Pham^{a,b} A. Toumi^{a,*} A. Turatsinze^a

4 ^a *LMDC, INSAT/UPS Génie Civil, 135 Avenue de Rangueil, 31077 Toulouse cedex 04*

5 *France*

6 ^b *Faculty of Bridge and Road Engineering, The University of Danang - University of*
7 *Science and Technology, 54 Nguyen Luong Bang Str., Danang, Vietnam*

8 **Abstract:** Bond defects at rubber-cement matrix interface are detrimental to durability
9 of the cement composite. Therefore, coating rubber aggregates with copolymer has been
10 suggested to overcome this defect. This paper aims to investigate the effect of an improved
11 rubber-cement matrix bond on frost resistance. Freeze-thaw temperature cycles were con-
12 trolled by a thermal sensor embedded inside the core of a mortar specimen. Measurements
13 of relevant quantities, such as mass loss, length change, mechanical properties (relative
14 dynamic modulus of elasticity, compressive and flexural strengths), and durability factor,

*corresponding author. E-mail address: toumi@insa-toulouse.fr (A. Toumi). Phone: (33 5 61 55 99 19)
LMDC, INSA/UPS Génie Civil, 135 Avenue de Rangueil, 31077 Toulouse Cedex 04 France.

15 demonstrated that rubberized cement-based materials were more resistant under freeze-
16 thaw environments than the control one. Especially, regardless of slight length gain of
17 mortar incorporating coated rubber aggregates, copolymer coating still made the compos-
18 ite durable in frost conditions owing to its improved strain capacity and higher residual
19 post-peak tensile strength.

20

21 **Keywords:** Rubber aggregates; rubber-cement matrix interface; rubber coating; freeze-
22 thaw resistance; durability factor; strain capacity.

23 1 Introduction

24 Rubber aggregates (RA) addition into cementitious mixtures was reported to improve
25 resistance of cement-based composites to freeze-thaw action [1–8]. Benazzouk et al. [1]
26 studied the frost behaviour of cement-rubber composites in which RA contents were rang-
27 ing from 0% to 40%. The authors reported a reduction in both mass loss and relative
28 dynamic modulus loss of the materials containing 30% and 40% of RA by volume, demon-
29 strating an improvement in frost resistance of the composites. According to Paine et al. [2],
30 6% volume of RA incorporation was suitable to improve frost durability in terms of resist-
31 ing scaling phenomenon and of limiting a decrease in relative dynamic modulus. However,
32 due to bond defects at rubber-cement matrix interface, performance of rubberized concrete
33 under freeze-thaw conditions appeared less impressive than that of the one manufactured

34 with a high content of air entrained [2]. Al-Akhras et al. [3] investigated relative dynamic
35 modulus of elasticity during freeze-thaw actions and reported that, compared to the con-
36 trol mortar, the ones incorporating rubber ash (size 0.15 mm) as natural sand replacement
37 at two distinct levels of 5% and 10% by weight exhibited higher durability factor, which
38 was determined according to ASTM C666/C666M standard [9]. It should be noted that
39 relative dynamic elastic modulus is defined as a variation in the dynamic modulus of the
40 specimens.

41 The detrimental effect of RA addition on freeze-thaw resistance of rubberized cement-
42 based composites was also reported. Karahan et al. [10] partially replaced natural sand
43 in self-consolidating concretes with RA (size 4.75-0.15 mm) at different RA contents of
44 0%, 10%, 20% and 30%, by volume. Their experimental results showed some spalling on
45 surface of rubberized concrete specimens, and a gradual loss in flexural strength and mass
46 was observed with an increase of rubber content. Similarly, according to investigations of
47 Savas et al. [11], increasing rubber volume would decrease the freeze-thaw durability of
48 rubberized concrete, which was measured according to ASTM C666/C666M standard [9]
49 using procedure A. Among previous studies, Richardson et al. [7] found that washing
50 RA before adding them to cementitious mixtures led to a composite with lower pulse
51 velocity but reduced weight loss under freeze-thaw conditions. As reported by Si et al. [12],
52 resistance of rubberized concrete to freeze-thaw environments appeared more significant in
53 composites incorporating 15% by volume of sodium-treated RA replacing fine aggregates
54 (rubber size 1.44 - 2.83 mm and 40-minute sodium treatment with the concentration of

55 4%), especially in terms of preventing both mass loss and relative dynamic elastic modulus
56 reduction.

57 As briefly summarized above, there is still no consensus about the role of RA in ce-
58 mentitious mixtures against freeze-thaw conditions. Also, all previous studies have only
59 evaluated durability of rubberized cement-based composites to frost actions thanks to mass
60 loss and changes in relative dynamic modulus of elasticity. Moreover, no investigations
61 have been assessed on bond effects between RA and cement matrix on freeze-thaw durabil-
62 ity of the composites. This study therefore aims to characterize freeze-thaw resistance of
63 two rubberized mortars, one of them incorporating polymer-coated RA, as demonstrated
64 by Pham et al. [13, 14], to obtain an enhanced RA-cement matrix interfacial transitional
65 zone. The mass loss, changes in ultrasonic pulse velocity and relative dynamic modulus
66 of elasticity, residual mechanical properties (compressive and flexural strengths), durabil-
67 ity factor, and especially length change of these mortars under freeze-thaw actions were
68 investigated and compared to the ones of control mortar.

69 **2 Materials and methods**

70 **2.1 Materials and mix proportions**

71 As mentioned earlier, control mortar and two rubberized ones were investigated. Materials
72 used for making these mortars include cement CEM I (52.5 R), natural sand (0-4 mm),
73 RA (similar size as sand), and water. It should be noted that, in these rubberized mortars,

only 30% volume of sand was replaced by RA. Compared to higher specific gravity (2.62) and significant water absorption (1.9%) of sand, RA have a lower density of 1.2 and are hydrophobic materials. These characteristics can explain a reduction in workability and segregation phenomena of rubberized cement-based mixtures. Hence, superplasticizer and viscosity agent were used to maintain workability and to make sure homogeneity of the composite, respectively. It is worth recalling that hydrophobic nature of RA is a main reason of higher porosity in rubberized cement-based composites due to air-entrapment effect when RA are in contact with mixing water. Obviously, bond defects at untreated rubber-cement matrix interface also contribute to such property. The difference in size distribution between RA and sand used in this work is described in Fig. 1.

Three mortars studied (control, untreated and coated rubberized ones) and their mix proportions are presented in Table 1. It should be noted that acronyms UR and CR denote Untreated Rubber and Coated RA, respectively; letter P stands for coPolymer, which is as bonding material to enhance the interfacial zone between RA and cement matrix. The rubber-cement matrix enhancement demonstrated in Fig. 2 was obtained using a coating method [14]. Firstly, RA were required to precoat with styrene-butadiene-type copolymer (2% mass of RA). The processed RA were then maintained in a conditioned room fixed at 20 °C temperature and at 50% relative humidity for 1 hour. This step is necessary for copolymer's condensation and stabilization on RA surface. Finally, pre-mixed cementitious mixture was prepared for a light and short mixing with coated RA.

Prismatic mortar specimens (40 mm x 40 mm x 160 mm) were prepared for freeze-

thaw test. For monitoring length change, during mould preparation and casting process, two steel pinholes were embedded at the center of two head ends of mortar specimens. Then 24 hours after casting, the specimens were demoulded and placed in the curing room maintained under controlled atmosphere (20 °C temperature and 95% relative humidity) for 27 days before starting freeze-thaw cycles.

2.2 Freeze-thaw test programme

The freeze-thaw resistance test of control and rubberized mortars was carried out according to NF P18-424 standard [15] in combination of ASTM C666/C666M-15 standard - Procedure A [9]. An environmental chamber is used to simulate freeze-thaw cycles. It is able to induce the highest and lowest temperatures, namely 150 °C and -40 °C.

In order to induce frost actions, temperature inside the chamber can be controlled by either a chamber sensor or the one embedded in the core of a specimen (Fig. 5). In this work, freeze-thaw cycles were established in accordance with the latter case. Actual temperatures in the chamber and at the core of a mortar specimen were recorded during the test. The temperature-controlled specimens illustrated in Fig. 3 were made of untreated rubberized mortar (30UR). The authors' experience showed that during casting and hardening process or under freeze-thaw actions, the thermal sensor embedded at the center of the temperature-controlled specimen can fail, stop to work and need to be replaced by another specimen. Hence, to prevent these hazards, several temperature-controlled specimens were prepared and placed in the chamber as tested specimens. The curing pro-

cess of such specimens was similar to the one of tested mortars. One should notice that the connecting systems including electronic wire lines and the sensor connectors must be protected under high moisture condition of curing.

Fig. 4 shows the temperature cycle set-up for the freeze-thaw test. The black, red, green colors indicate the target freeze-thaw temperature, and the ones of the chamber and at the core of the control specimen, respectively. The actual core temperature was dropped from 4 ± 2 °C to -18 ± 2 °C for around 3.0 hours, kept at -18 ± 2 °C for 0.5 hour, raised from -18 ± 2 °C to 4 ± 2 °C for other 2.0 hours, and kept at 4 ± 2 °C for 0.5 hour. The duration of a freeze-thaw cycle was 6 hours. It therefore allowed 4 cycles per day to be conducted. This core temperature cycle obtained was quite adapted to the requirement of standards [9,15]. Indeed, it was difficult to set up the core temperature of the controlled specimen close to the one inside the chamber due to requirement of thermal conductivity time into mortar specimens.

The arrangement of mortar specimens in the chamber is shown in Fig. 5. Before transferring the specimens into the chamber, the initial length, mass, and ultrasonic pulse velocity of prismatic mortar specimens were measured. Compressive and flexural tests were also carried out in order to determine initial strengths. It should be noted that the specimens were required to dry carefully using a sponge to remove only surface water before weight measurement. In general, the freeze-thaw test is continuing until the mortar specimens have been subjected to 300 cycles or terminated earlier if the relative length change overpasses $500 \mu m/m$ [14] or $1000 \mu m/m$ [9]; or the relative dynamic modulus of

elasticity falls below 60%, as recommended in standards [9, 15]. In this study, the test was finalized when the expansion of mortar specimens exceeds 0.1% ($1000 \mu m/m$) of its original dimension.

After a given number of freeze-thaw cycles, length change, mass loss, ultrasonic pulse velocity were measured. Flexural and compressive tests on the prismatic mortar specimens were only performed at 130 cycles and at the test end. Details of necessary tests are described as below.

2.2.1 Mass loss and length changes

During the freeze-thaw test, the specimen mass was simply measured by weighing the surface-dried specimens using a scale with an accuracy of 0.01 g. The mass loss is determined according to Eq. (1), where m_o and m_i are weights before starting freeze-thaw test and after i cycles of freezing and thawing, respectively. A length sensor with a precision of $1 \mu m$ was used for determining the length of mortar specimens. Length gain (dimensional expansion) is then calculated according to Eq. (2), where L_1 , L_i are the readings on the length sensor at the beginning of the test and at the i_{th} freeze-thaw cycle, respectively; and L_0 is the initial distance between two steel pinholes (specimen length of 160 mm). The average mass loss and length change from three specimens of each mortar were reported.

$$Mass\ loss\ (\%) = \frac{m_0 - m_i}{m_0} \cdot 100 \quad (1)$$

153

$$Length\ gain\ (\mu m/m) = \frac{L_i - L_1}{L_0} \quad (2)$$

154 **2.2.2 Ultrasonic pulse velocity test**

155 The ultrasonic pulse velocity was determined according to NF EN 12504-4 standard [16].
 156 The tester used mainly consists of a control unit (an electrical pulse generator, an am-
 157 plifier, and an electronic timing device) and a pair of transducers. The devices with a
 158 frequency of 54 kHz are used to generate an ultrasonic pulse to travel on the path length
 159 of 160 mm from the transmitting transducer to the receiving one. The apparatus must be
 160 calibrated at every testing time using a calibration bar. The time duration for acoustic
 161 wave to propagate through the longitudinal direction of the specimen and the ultrasonic
 162 pulse velocity were recorded. Three specimens of each mortar type and at least five
 163 measurements for each specimen were taken to make sure that the variation between the
 164 measured transit time on single tested specimen should be within $\pm 1\%$ of the mean value
 165 of these three measurements. Note that the specimen surface contacted with transducers
 166 must be smooth enough by coating a quick-setting epoxy resin, especially when mortars
 167 are subjected to damage after a given number of freeze-thaw cycles.

168 From values of ultrasonic pulse velocity, a relative dynamic modulus of elasticity (P_c)
 169 is calculated as Eq. (3) [17], where v_c and v_o are ultrasonic pulse velocities at the c_{th} cycle
 170 of freezing and thawing and at time right before starting freeze-thaw test, respectively.
 171 The durability factor (DF) is finally determined at the end of freeze-thaw test using Eq.

172 (4), as recommended by ASTM C666/C666M-15 standard [9].

$$P_c (\%) = \frac{v_c^2}{v_0^2} \cdot 100 \quad (3)$$

173

$$DF = \frac{P \cdot N}{M} \quad (4)$$

174 where P (%) is relative value of dynamic elastic modulus at N^{th} cycle; N is the number of
175 freeze-thaw cycles at which P drops to the minimum value for terminating the frost test
176 (60% as required by standards [9, 15]) or the selected number of freeze-thaw cycles when
177 frost actions are to be ended (whichever is less); and M is the specific number of cycles at
178 the end of freeze-thaw test.

179 **2.2.3 Flexural and compressive tests**

180 The flexural and compressive tests were carried out on prism mortar specimens according
181 to NF EN 1015-11 standard [18]. Firstly, three point-bending tests were carried out on
182 prismatic mortar specimens to get load-bearing capacity. The two rollers of the flexural
183 tests were spaced at a distance of 100 mm. Two parts of specimens obtained after the
184 bending tests were then compressed on an area of 40 mm x 40 mm to obtain the compres-
185 sive strength. The loading rates of flexural and compressive tests were 0.05 kN/s and 0.5
186 kN/s, respectively.

3 Results and discussion

3.1 Mass loss

Fig. 6 shows mass loss versus number of freeze-thaw cycles for three types of mortars. The untreated rubberized mortar specimens were observed to increase slightly in mass for the first 50 cycles of freezing and thawing. It is due to the higher air-void density of this mortar, which still absorbs water to reach a critical degree of saturation [12]. The mass of the control mortar specimens started to decrease quickly since the 160th cycles of freezing and thawing, and to become severely deteriorated at approximately 200 cycles compared to other rubberized mortar specimens (Fig. 7). A slight difference in mass loss was also observed between rubberized mortar using untreated RA and the one incorporating copolymer coated RA.

3.2 Length gain

The expansion of all mortar specimens under the freeze-thaw action is illustrated in Fig. 8. It can be clearly seen that the length gain of control mortar is much higher than the one of rubberized mortars. The smaller length change of rubberized mortar specimens exposed to freeze-thaw cycles can be explained as below:

- (i) As demonstrated from Scanning Electron Microscope (SEM) observations and air permeability values from the same composites [13, 14], incorporation of RA in cementitious mixture induces high porosity not only at the poor rubber-cement matrix

206 interface, but also especially high density of air pores in the core of cementitious
 207 matrix. It means that many escape spaces are formed in rubberized mortars. As
 208 explained by Mehta et al. [19], much lower temperature was required to freeze water
 209 in capillary pores than the one in gel pores. Higher energy state in gel pores forces
 210 water to transport to the capillary ones in order to balance the energy between
 211 these pores. Therefore, such escape spaces in rubberized cement-based composites
 212 play an important role to reduce energy gradient, leading to a decrease in expansion
 213 of rubberized mortars. Normally, spacing factor, a parameter associated with the
 214 distance from the periphery of an air void to adjacent ones in cementitious matrix
 215 measured on microscopic scanning pictures of air-void system according to ASTM
 216 C457/C457M [20] is used to estimate whether the cement-based composites are re-
 217 sistant to freeze-thaw actions [21]. However, due to unexpected problems related
 218 to polishing procedure of rubberized mortar specimens, spacing factor is therefore
 219 difficult to qualify accurately [11]. Additional voids would be generated due to low
 220 stiffness of RA and bond defects available at untreated rubber-cement matrix inter-
 221 face.

222 (ii) It is necessary to recall that low stiff RA should help in absorbing energy induced by
 223 a given damage process [22]. Hence, compared to the control mortar, high amount of
 224 energy from freeze-thaw actions in rubberized composites is assumed to be released.

225 (iii) Low water porosity and capillary absorption of rubberized cement-based composites

226 compared to the control one can reduce the volume change due to ice formation.
227 Moreover, high water absorption of natural aggregates (sand) is also detrimental to
228 the durability under freeze-thaw performance than RA that do not absorb water.

229 (iv) According to Sahmaran et al. [23], tensile strain capacity and strain-hardening be-
230 haviour were also important to prevent damage from freeze-thaw actions. As demon-
231 strated by previous authors [24–26], low stiffness property of RA is beneficial to im-
232 prove strain capacity, the deformation at failure of rubberized cement-based compos-
233 ites, and to result in higher residual post-peak tensile strength. Hence, freeze-thaw
234 resistance of rubberized mortars was consequently improved.

235 The difference in length change between rubberized mortar incorporating untreated
236 RA and the one using coated RA was also observed. Rubberized mortars incorporating
237 coated RA exhibited a slightly higher expansion. It can be explained by the fact that
238 rubber coating resulted in an improved rubber-cement matrix bond and a partial reduction
239 in gel and capillary pores in the composite. The frost resistance of mortar specimens can
240 be evaluated through the total number of freeze-thaw cycles at which the relative length
241 change exceeds $500 \mu m/m$ [15] or 0.1% of the original length [9]. As illustrated in Fig. 8
242 and Table 2, it can be concluded that rubberized mortars are more resistant to freeze-thaw
243 environments in term of length change due to a tolerance towards a greater number of
244 freeze-thaw cycles.

245 3.3 Ultrasonic pulse velocity

246 The ultrasonic pulse velocity of mortar specimens over a freeze-thaw test period is pre-
247 sented in Fig. 9. The initial ultrasonic pulse velocities of rubberized mortars after 28 days
248 in the curing room were lower than the one of control mortar. Higher density of pores
249 in the cement matrix due to air entrapment phenomenon during casting process of rub-
250 berized cementitious mixtures, bond defects at untreated rubber-cement matrix interface,
251 and low density of the composite are qualified explanations why the transmitting time of
252 ultrasonic pulse waves in rubberized mortars is delayed, leading to low pulse velocity of
253 rubberized mortars.

254 Under frost actions, the pulse velocity of all mortar specimens remained similarly
255 as original values over the first 50 cycles of freezing and thawing. After this period,
256 while pulse velocity of rubberized mortars seemed to be still constant, the one of control
257 mortar decreased gradually and reached the value lower than the one of rubberized mortars
258 after approximately 180 cycles of freezing and thawing. This is a consequence of damage
259 induced by ice pressure inside the control mortar. On the contrary, presence of RA can
260 absorb energy induced by volumetric expansion during phase change of water. Therefore,
261 control mortar was less durable than the rubberized mortars, which highlighted the greater
262 relevance of the pores induced by presence of RA in the composites. Coating RA with
263 copolymer seemed to have no specific effect on a change of pulse velocity during a 200
264 freeze-thaw cycle testing period.

265 Based on ultrasonic pulse velocity, cement-based materials can be classified as excellent,

266 good, questionable, poor and very poor qualities [27]. One found that initial pulse velocity
267 values of all control and rubberized mortars were greater than 3660 m/s and less than
268 4575 m/s, thus classifying them as good mortars. At the end of freeze-thaw test, while
269 rubberized mortars still remained their original classification, the control mortar dropped
270 to a lower standard, a questionable one.

271 The number of freeze-thaw cycles where relative dynamic modulus of elasticity falls
272 below 60% is also considered as a parameter to express the frost resistance of mor-
273 tar/concrete [9]. Fig. 10 presents the relative dynamic modulus of elasticity over a period
274 of 200 cycles of freezing and thawing. It can be clearly seen that none of control mortar
275 specimens was freeze-thaw resistant after 200 cycles. On the contrary, rubberized mortar
276 specimens exhibited a very good performance under frost action. Durability factor (DF)
277 determined at the test end for three types of mortars is compared in Table 2. Based on
278 durability factor values, Hansen [28] reported that freeze-thaw resistance of cement-based
279 composites can be classified as follows: Nonresistance to freeze-thaw actions ($DF \leq 40\%$),
280 doubtful frost resistance ($40\% < DF \leq 60\%$), acceptable frost resistance ($60\% < DF \leq 80\%$),
281 and frost resistance ($DF > 80\%$). Therefore, it can be concluded that incorporating 30%
282 volume of RA (0 - 4 mm) to cementitious mortars as a sand replacement produced "frost
283 resistance" of rubberized mortars compared the "doubtful frost resistance" of the control
284 one.

285 3.4 Loss of compressive and flexural strengths

286 The residual compressive and flexural strengths after 130 freeze-thaw cycles and at the
287 test end are presented in Figs. 11 and 12, respectively. One should note that zero values
288 of such mechanical properties of the control mortar at the test end because of a serve
289 deterioration on the surface of the specimens. At the 130th cycle of freezing and thawing,
290 compressive and flexural strengths of the control mortar were decreased by 33% and 31%,
291 respectively. Despite low expansion and insignificant change in pulse velocity of untreated
292 rubberized mortar specimens, a slight reduction in compressive and flexural strengths
293 of this type of mortar was still observed. It can be attributed to the additional water
294 absorption of untreated rubberized mortar during the first period of freeze-thaw action.
295 The enhanced bond between RA and cement matrix was observed to maintain mechanical
296 properties (flexural and compressive strengths) with increasing the number of freeze-thaw
297 cycles. It is explained by Sahmaran et al. [23] that, in addition to the air-void system,
298 other parameters such as high tensile strain capacity and strain-hardening behaviour of
299 cement-based composites are important for resisting cycles of freezing and thawing. As
300 reported by Pham et al. [13, 14], coating RA with copolymer before mixing them with
301 cementitious mixture was demonstrated to improve strain capacity and residual post-peak
302 tensile strength compared to the untreated one. Therefore, the coated rubberized mortar
303 was still durable under freeze-thaw cycles regardless of a slight length gain as reported
304 above.

305 4 Conclusions

306 Freeze-thaw resistance of rubberized mortars were investigated and compared to the one
307 of control mortar. From experimental results, the following conclusions can be drawn:

- 308 • Rubberized cement-based composites were more resistant to frost environments than
309 the control one. It was especially validated based on the length change.
- 310 • Durability of rubberized mortars under freeze-thaw conditions can be attributed to
311 high energy absorption and hydrophobic nature of RA and to lower water capillary
312 absorption, high strain capacity and better residual post-peak performance of the
313 composites.
- 314 • Rubber coating to enhance rubber-cement matrix interface led to a slight increase
315 in length change of coated rubberized mortar under freeze-thaw actions, but the
316 composite was still more durable than the control mortar under frost environment.

317 References

- 318 [1] A. Benazzouk and M. Queneudec. Durability of cement-rubber composites under
319 freeze thaw cycles. In *Proceeding of International congress of Sustainable Concrete*
320 *Construction, Dundee-Scotland*, pages 355–362, 2002.
- 321 [2] K.A. Paine, R.K. Dhir, R. Moroney, and K. Kopasakis. Use of crumb rubber to achieve
322 freeze/thaw resisting concrete. In *Challenges of Concrete Construction: Volume 6*,

- 323 *Concrete for Extreme Conditions: Proceedings of the International Conference held*
 324 *at the University of Dundee, Scotland, UK on 9–11 September 2002*, pages 485–498.
 325 Thomas Telford Publishing, 2002.
- 326 [3] N.M. Al-Akhras and M.M. Smadi. Properties of tire rubber ash mortar. *Cement and*
 327 *concrete composites*, 26(7):821–826, 2004.
- 328 [4] İ.B. Topçu and A. Demir. Durability of rubberized mortar and concrete. *Jour-*
 329 *nal of materials in Civil Engineering*, 19(2):173–178. DOI: 10.1061/(ASCE)0899–
 330 1561(2007)19:2(173), 2007.
- 331 [5] P. Turgut and B. Yesilata. Physico-mechanical and thermal performances of newly
 332 developed rubber-added bricks. *Energy and Buildings*, 40(5):679–688, 2008.
- 333 [6] K.A. Paine and R.K. Dhir. Research on new applications for granulated rubber in
 334 concrete. *Proceedings of the institution of civil engineers: construction materials*,
 335 163(1):7–17, 2010.
- 336 [7] A.E. Richardson, K.A. Coventry, and G. Ward. Freeze/thaw protection of concrete
 337 with optimum rubber crumb content. *Journal of Cleaner Production*, 23(1):96–103.
 338 DOI: 10.1016/j.jclepro.2011.10.013, 2012.
- 339 [8] M. Gesoğlu, E. Güneyisi, G. Khoshnaw, and S. İpek. Abrasion and freezing-thawing
 340 resistance of pervious concretes containing waste rubbers. *Construction and Building*
 341 *Materials*, 73:19–24. DOI: 10.1016/j.conbuildmat.2014.09.047, 2014.

- [9] ASTM C666/C666M-15. Standard test method for resistance of concrete to rapid freezing and thawing. *ASTM Int. West Conshohocken, PA*, 2015.
- [10] O. Karahan, E. Özbay, K. Hossain, M. Lachemi, and C.D. Atiş. Fresh, mechanical, transport, and durability properties of self-consolidating rubberized concrete. *ACI Materials Journal*, 109(4), 2012.
- [11] B. Savas, S. Ahmad, and D. Fedroff. Freeze-thaw durability of concrete with ground waste tire rubber. *Transportation Research Record: Journal of the Transportation Research Board*, (1574):80–88. DOI: 10.3141/1574–11, 1997.
- [12] R. Si, S. Guo, and Q. Dai. Durability performance of rubberized mortar and concrete with naoh-solution treated rubber particles. *Construction and Building Materials*, 153:496–505. DOI: 10.1016/j.conbuildmat.2017.07.085, 2017.
- [13] N.P. Pham, A. Toumi, and A. Turatsinze. Effect of styrene-butadiene copolymer coating on properties of rubberized cement-based composites. In *V. Mechtcherine, V. Slowik, P. Kabele (Eds.), Strain-Hardening Cem. Compos. SHCC4, Springer Netherlands, Dordrecht*, pages 342–350. DOI:10.1007/978–94–024–1194–2–40., 2018.
- [14] N-P. Pham, A. Toumi, and A. Turatsinze. Rubber aggregate-cement matrix bond enhancement: Microstructural analysis, effect on transfer properties and on mechanical behaviours of the composite. *Cement and Concrete Composites*, 94:1–12. DOI: 10.1016/j.cemconcomp.2018.08.005, 2018.

- [15] NF P18-424. *Concrete - Freeze test on hardened concrete - Freeze in water - Thaw in water*, 2008.
- [16] NF EN 12504-4. *Testing concrete. Part 4: Determination of ultrasonic pulse velocity*, 2005.
- [17] R. Pleau and M. Pigeon. *Durability of concrete in cold climates*. CRC Press, 2014.
- [18] NF EN 1015-11. *Methods of test for mortar for masonry. Part 11: Determination of flexural and compressive strength of hardened mortar*, 2000.
- [19] P.K. Mehta and P.J.M. Monteiro. *Concrete: Microstructure, properties, and materials*, fourth ed., McGraw-Hill Education, 2014.
- [20] ASTM C457 / C457M-16. Standard test method for microscopical determination of parameters of the air-void system in hardened concrete. *ASTM Int. West Conshohocken, PA*, 2016.
- [21] P.C. Aitcin. The durability characteristics of high performance concrete: a review. *Cement and concrete composites*, 25(4-5):409–420. DOI: 10.1016/S0958-9465(02)00081-1, 2003.
- [22] A.C. Ho, A. Turatsinze, R. Hameed, and D.C. Vu. Effects of rubber aggregates from grinded used tyres on the concrete resistance to cracking. *Journal of Cleaner Production*, 23(1):209–215. DOI:10.1016/j.jclepro.2011.09.016., 2012.

- [23] M. Şahmaran, M. Lachemi, and V. Li. Assessing the durability of engineered cementitious composites under freezing and thawing cycles. In *Recent Advancement in Concrete Freezing-Thawing (FT) Durability*. ASTM International, 2010.
- [24] A. Turatsinze, S. Bonnet, and J.L. Granju. Mechanical characterisation of cement-based mortar incorporating rubber aggregates from recycled worn tyres. *Build. Environ.*, 40:221–226. DOI:10.1016/j.buildenv.2004.05.012., 2005.
- [25] A. Turatsinze, J.L. Granju, and S. Bonnet. Positive synergy between steel-fibres and rubber aggregates: Effect on the resistance of cement-based mortars to shrinkage cracking. *Cem. Concr. Res.*, 36:1692–1697. DOI:10.1016/j.cemconres.2006.02.019., 2006.
- [26] A. Turatsinze and M. Garros. On the modulus of elasticity and strain capacity of self-compacting concrete incorporating rubber aggregates. *Resour. Conserv. Recycl.*, 52:1209–1215. DOI:10.1016/j.resconrec.2008.06.012., 2008.
- [27] V.M. Malhotra. *Testing hardened concrete: Nondestructive methods*. Number 9. Iowa State Press, 1976.
- [28] T.C. Hansen. *Recycling of demolished concrete and masonry*. CRC Press, 2014.

List of Figures

1	Difference in size distribution between sand and RA	23
---	---	----

397	2	Effect of copolymer coating on rubber-cementitious matrix interface: (a)	
398		bond defects (UR-Untreated RA), and (b) bond enhancement between ce-	
399		mentitious matrix (C) and coated RA (CR-P) [14]	24
400	3	Preparation of temperature-controlled specimens with thermal sensors . . .	25
401	4	Freeze-thaw temperature cycle set-up	26
402	5	Specimen arrangement in freeze-thaw chamber (unit: mm)	27
403	6	Comparison in mass loss between control and rubberized mortars	28
404	7	Degradation of mortar specimens at test end	29
405	8	Length changes versus number of freeze-thaw cycles	30
406	9	Changes of ultrasonic pulse velocity versus freeze-thaw cycles	31
407	10	Relative dynamic modulus of elasticity versus freeze-thaw cycles	32
408	11	Compressive strength versus freeze-thaw cycles	33
409	12	Flexural strength versus freeze-thaw cycles	34

410 List of Tables

411	1	Mix design and proportions (values in kg/m^3)	35
412	2	Frost resistance of mortar specimens	36

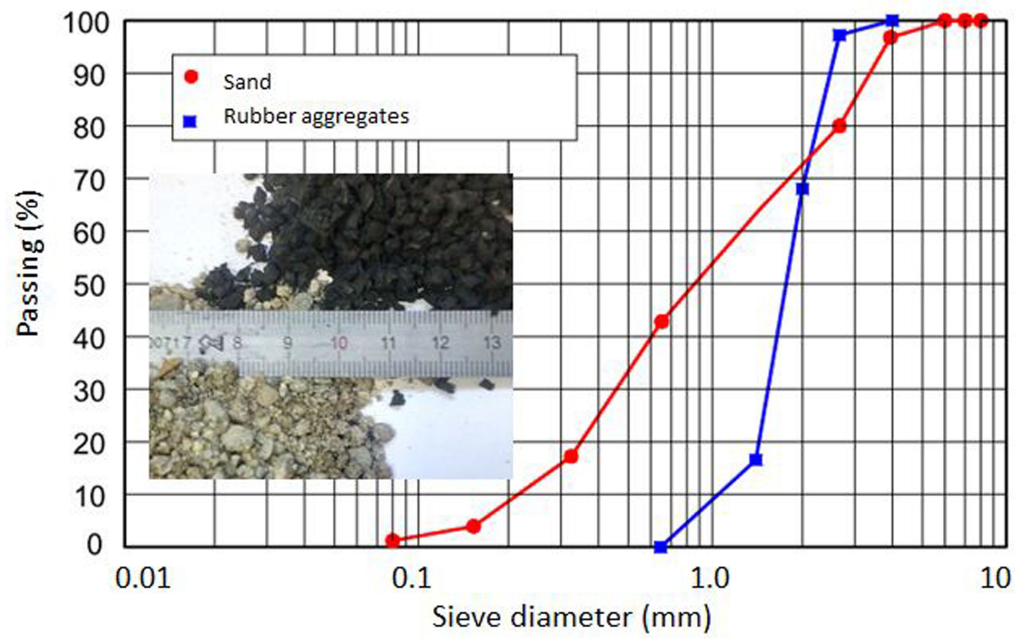


Figure 1: Difference in size distribution between sand and RA

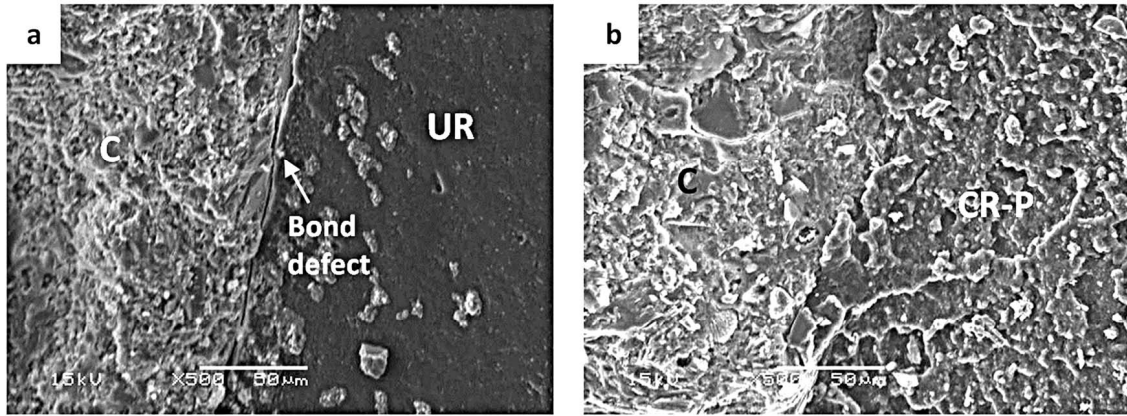


Figure 2: Effect of copolymer coating on rubber-cementitious matrix interface: (a) bond defects (UR-Untreated RA), and (b) bond enhancement between cementitious matrix (C) and coated RA (CR-P) [14]

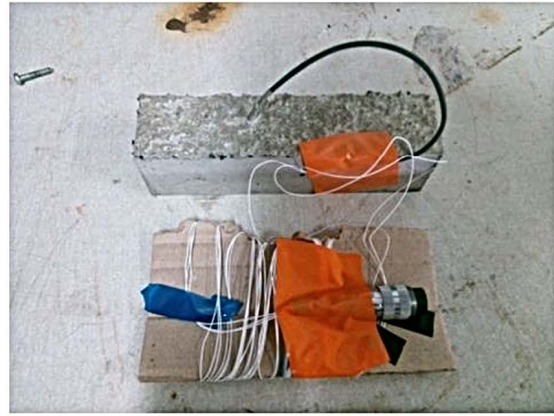
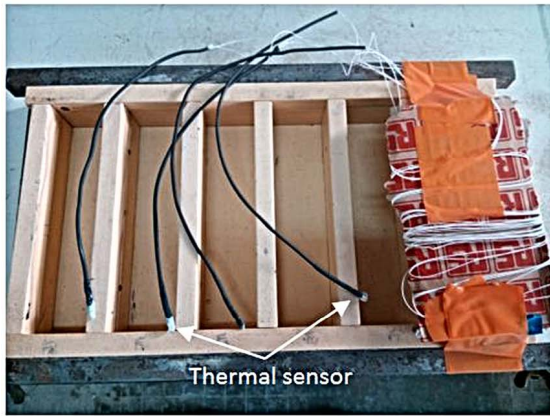


Figure 3: Preparation of temperature-controlled specimens with thermal sensors

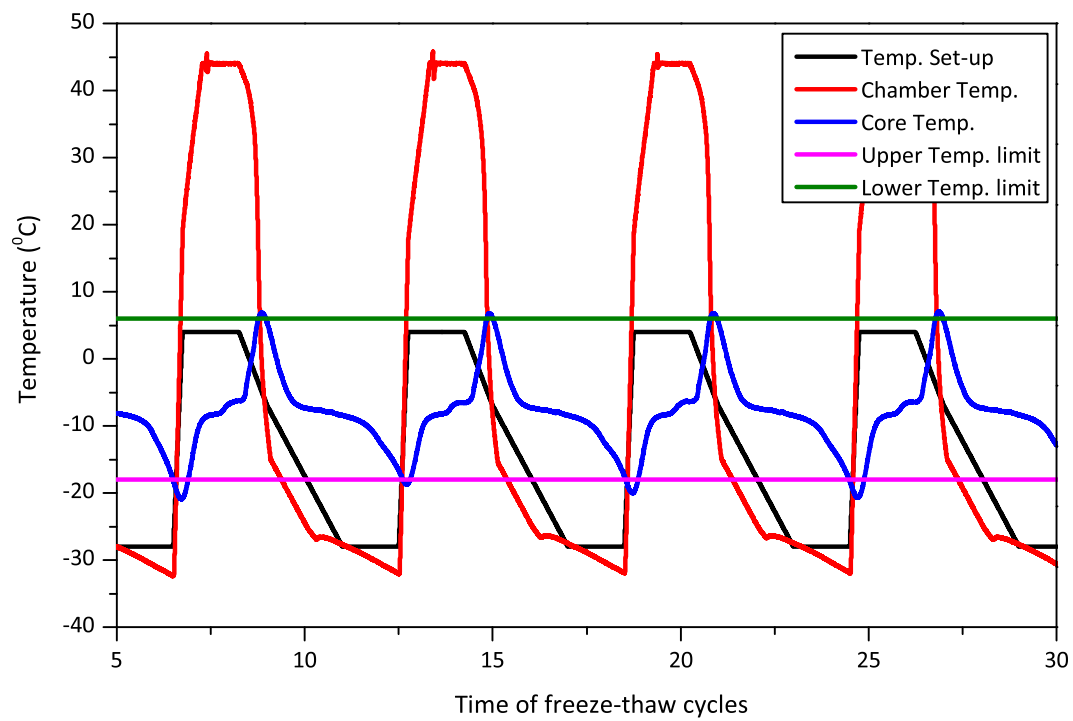


Figure 4: Freeze-thaw temperature cycle set-up

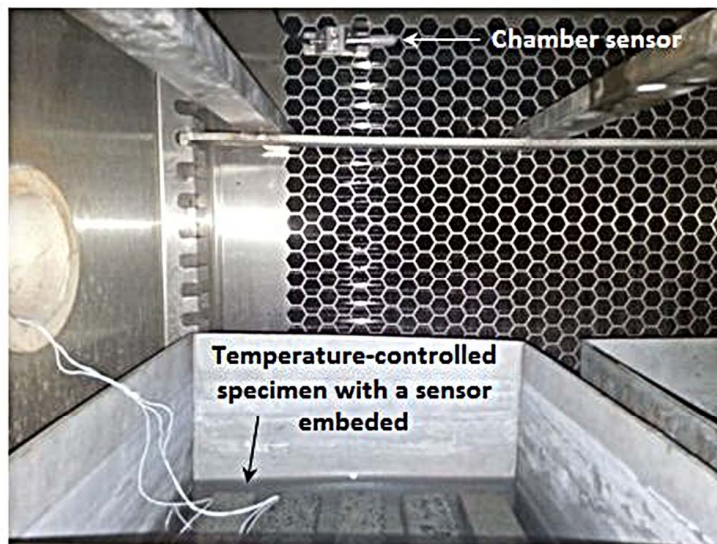
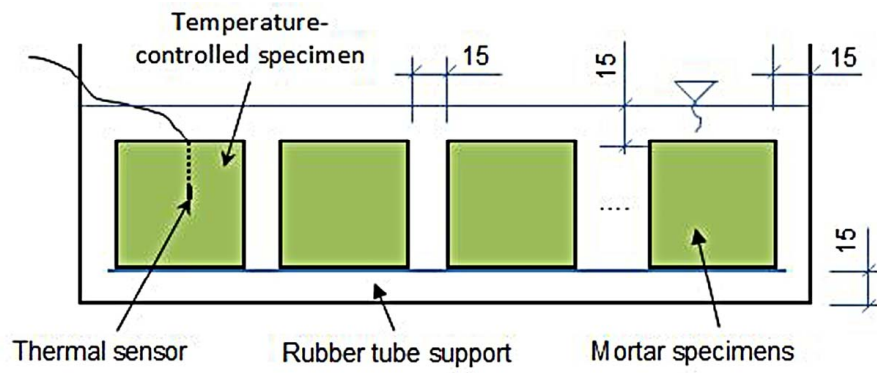


Figure 5: Specimen arrangement in freeze-thaw chamber (unit: mm)

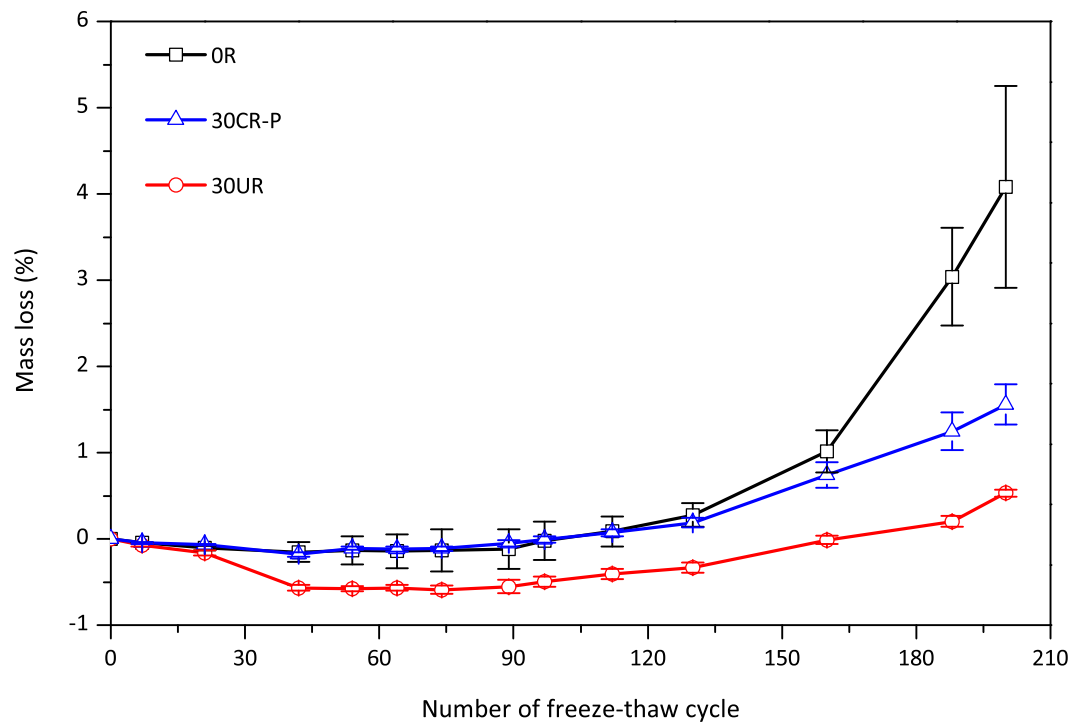


Figure 6: Comparison in mass loss between control and rubberized mortars

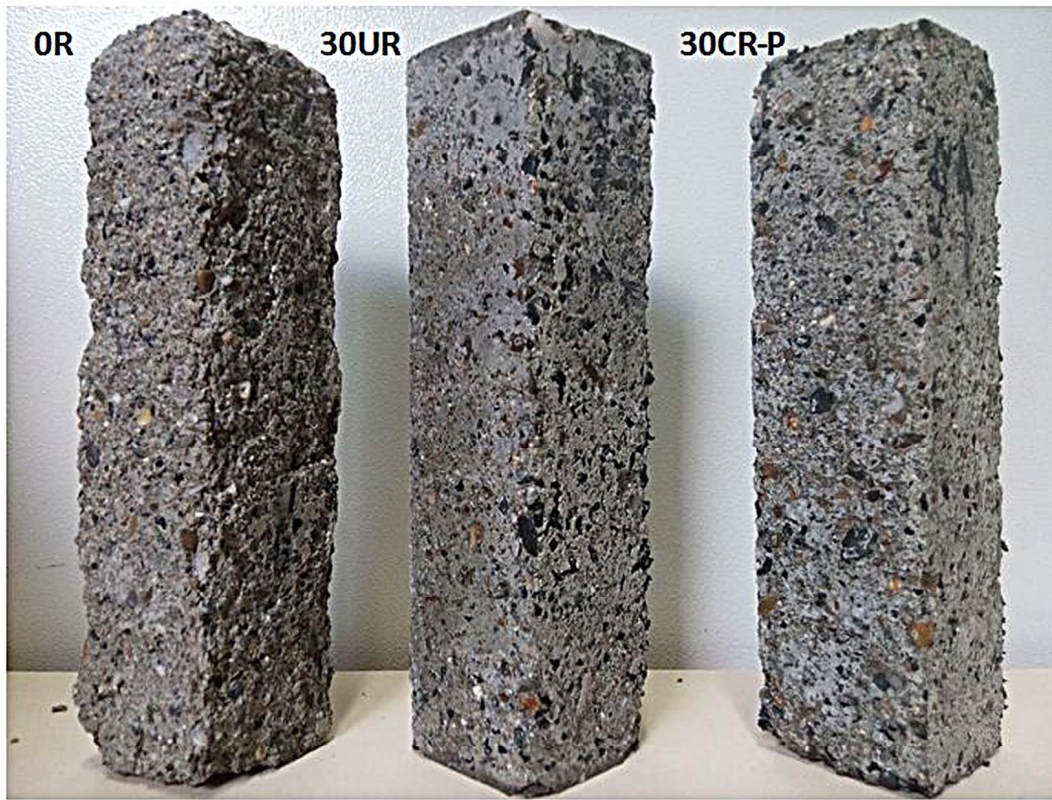


Figure 7: Degradation of mortar specimens at test end

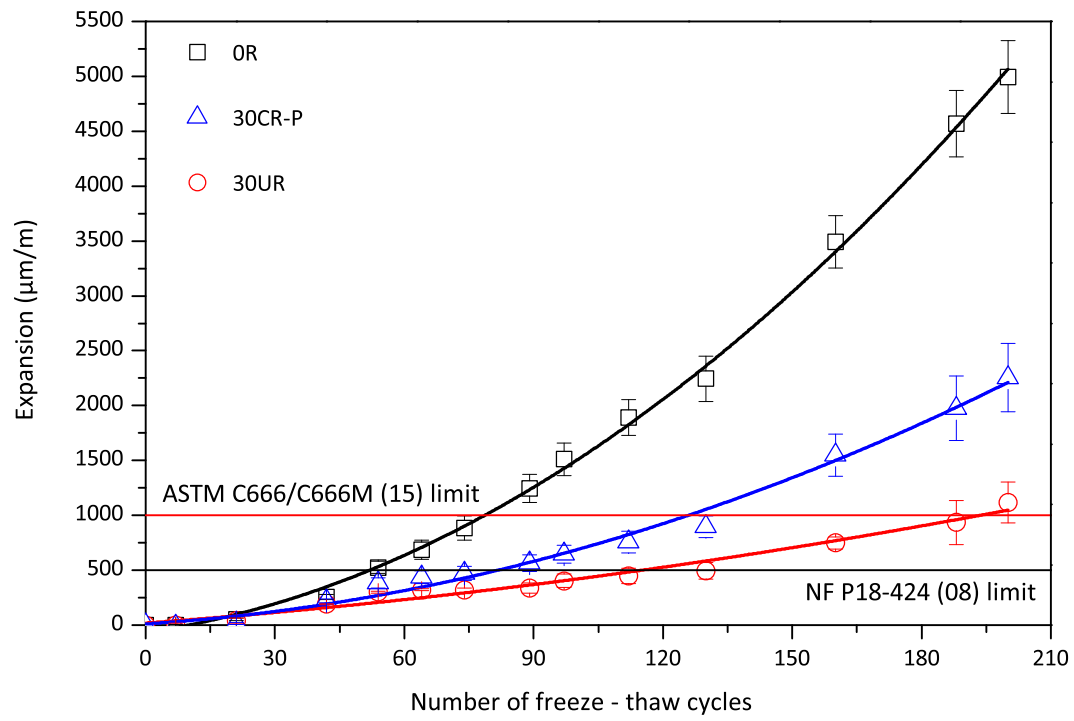


Figure 8: Length changes versus number of freeze-thaw cycles

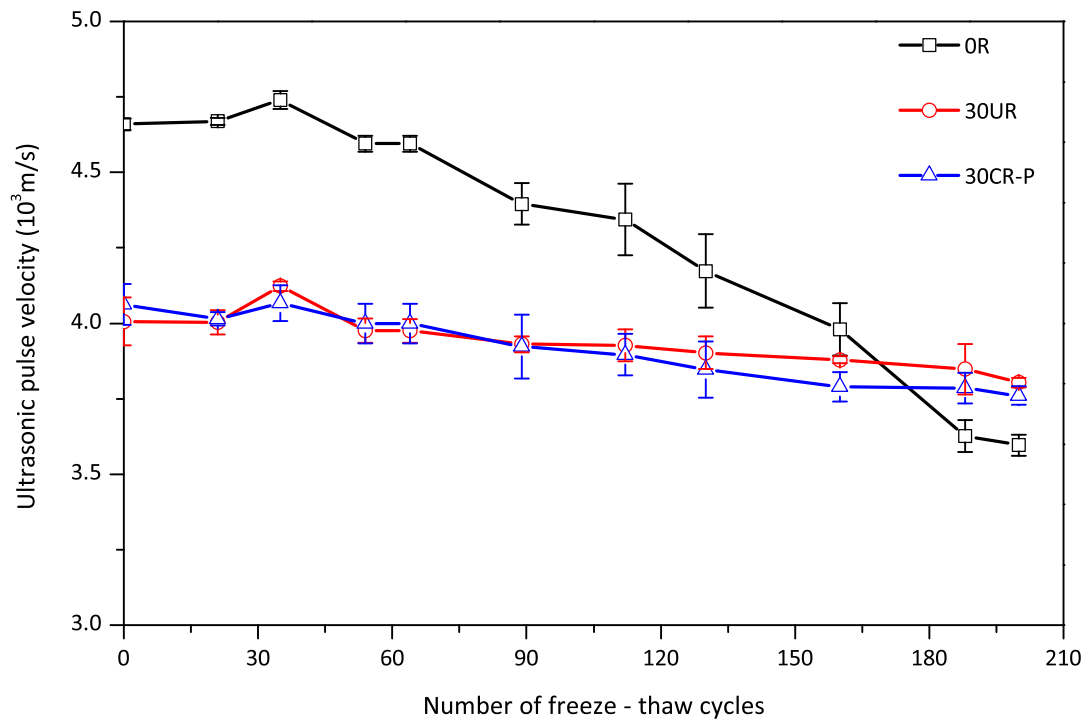


Figure 9: Changes of ultrasonic pulse velocity versus freeze-thaw cycles

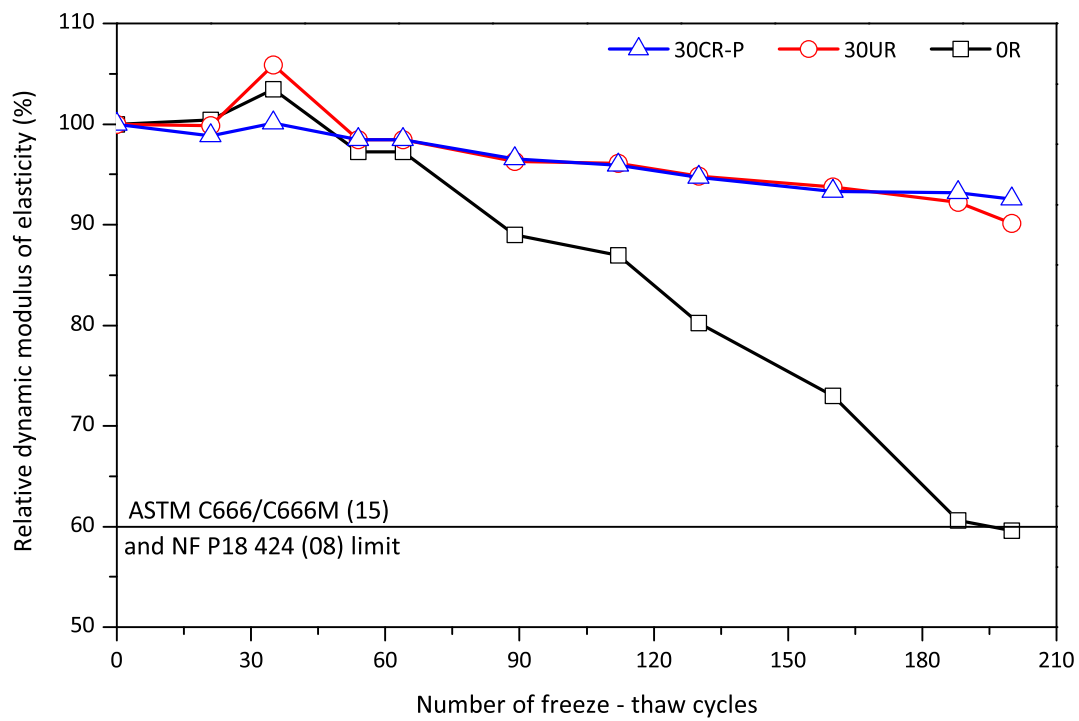


Figure 10: Relative dynamic modulus of elasticity versus freeze-thaw cycles

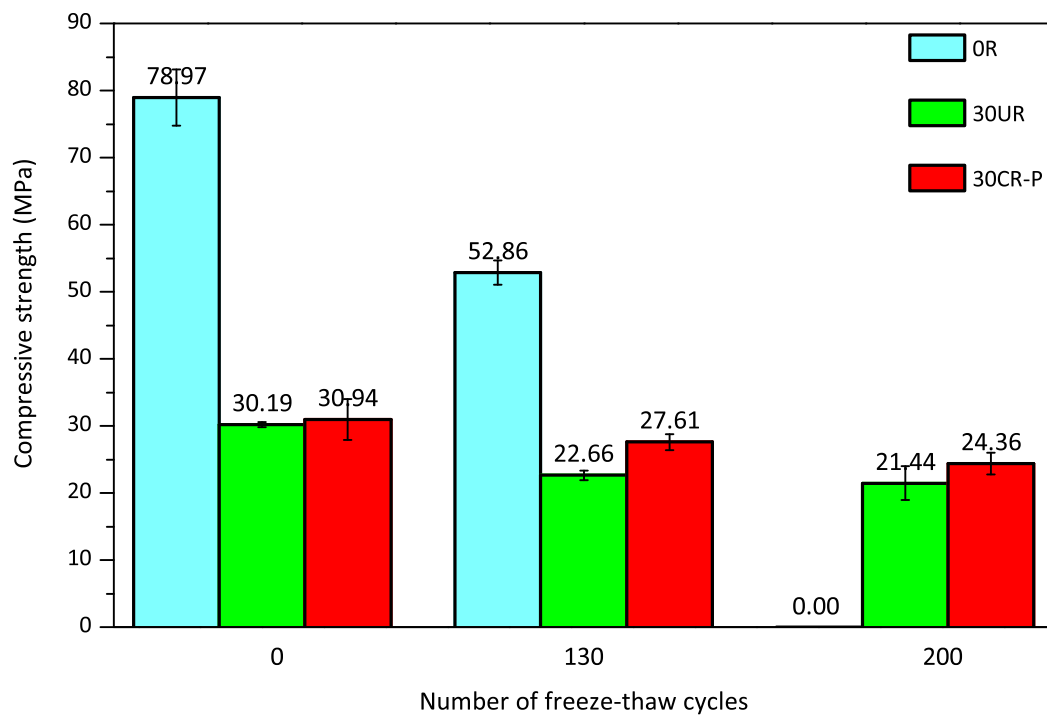


Figure 11: Compressive strength versus freeze-thaw cycles

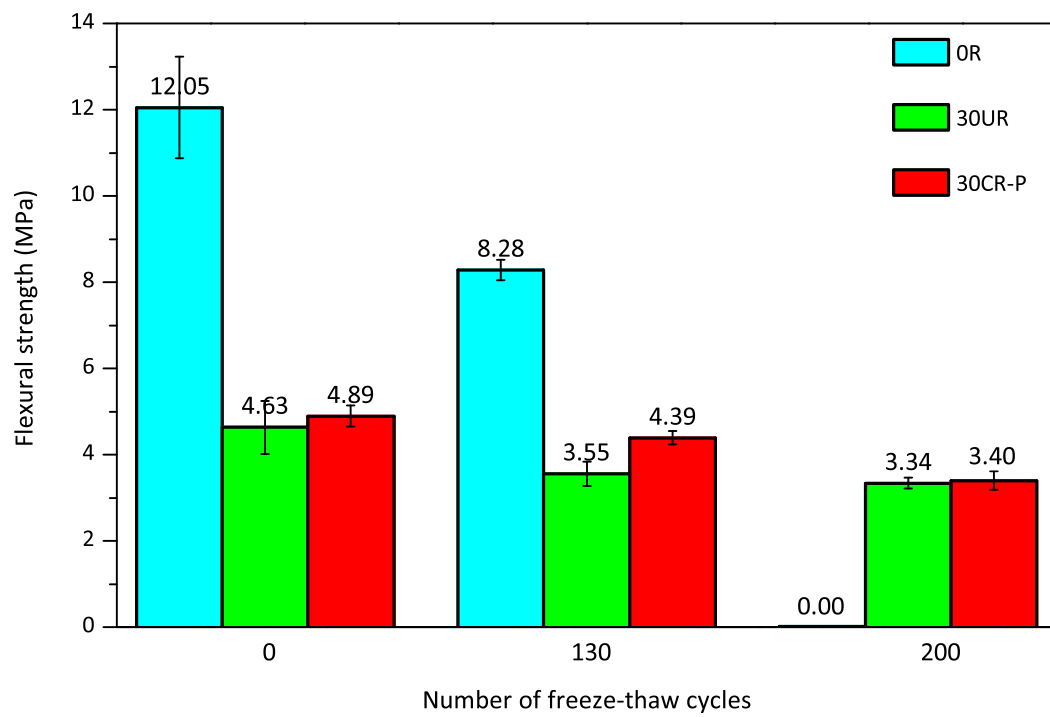


Figure 12: Flexural strength versus freeze-thaw cycles

Table 1: Mix design and proportions (values in kg/m^3)

Mix name	Cement	Sand	Water	RA	Superplasticiser	Viscosity agent
0R	500	1600	235	-	3.25	0.9
30UR	500	1120	235	220	3.25	0.9
30CR-P	500	1120	235	220	3.25	0.9

Table 2: Frost resistance of mortar specimens

Mix name	0R	30UR	30CR-P
Number of freeze-thaw cycles at limited length change (cycles)			
- Overpassing $500 \mu m/m$ [15]	51.95	115.12	81.69
- Exceeding 0.1% of original length [9]	78.63	193.63	125.84
Relative dynamic modulus of elasticity at test end (%)	59.6	90.1	92.6
Durability factor (%)	59.6	90.1	92.6
Freeze-thaw durability [28]	Doubtful	Frost resis- tant	Frost resis- tant